bioRxiv preprint doi: https://doi.org/10.1101/091330; this version posted December 5, 2016. The copyright holder for this preprint (which was not certified by peer review) is the author/funder, who has granted bioRxiv a license to display the preprint in perpetuity. It is made available under aCC-BY 4.0 International license.

Cross-tissue integration of genetic and epigenetic data offers insight into autism spectrum disorder

Shan V. Andrews[1,2], Shannon E. Ellis[3], Kelly M. Bakulski[4], Brooke Sheppard[1,2], Lisa A. Croen[5], Irva Hertz-Picciotto[6,7], Craig J. Newschaffer[8,9], Andrew P. Feinberg[10,11], Dan E. Arking[2,3], Christine Ladd-Acosta[1,2,10*], M. Daniele Fallin[2,10,12*]

[1]Department of Epidemiology, Johns Hopkins Bloomberg School of Public Health, Baltimore, MD, USA

[2]Wendy Klag Center for Autism and Developmental Disabilities, Johns Hopkins Bloomberg School of Public Health, Baltimore, MD, USA

[3]McKusick-Nathans Institute of Genetic Medicine, Johns Hopkins School of Medicine, Baltimore, MD, USA

[4]Department of Epidemiology, University of Michigan School of Public Health, Ann Arbor, MI, USA

[5]Division of Research, Kaiser Permanente Northern California, Oakland, CA, USA

[6]Department of Public Health Sciences, School of Medicine, University of California Davis, Davis, CA, US

[7]MIND Institute, University of California Davis, Sacramento, CA, USA

[8]AJ Drexel Autism Institute, Drexel University, Philadelphia, PA, USA

[9]Department of Epidemiology and Biostatistics, Drexel University Dornsife School of Public Health, Philadelphia, PA, USA

[10]Center for Epigenetics, Institute for Basic Biomedical Sciences, Johns Hopkins School of Medicine, Baltimore, MD, USA

bioRxiv preprint doi: https://doi.org/10.1101/091330; this version posted December 5, 2016. The copyright holder for this preprint (which was not certified by peer review) is the author/funder, who has granted bioRxiv a license to display the preprint in perpetuity. It is made available under aCC-BY 4.0 International license.

[11]Department of Medicine, Johns Hopkins School of Medicine, Baltimore, MD, USA

[12]Department of Mental Health, Johns Hopkins Bloomberg School of Public Health, Baltimore, MD USA

ABSTRACT

Epigenetics is an emerging area of investigation for Autism Spectrum Disorder (ASD). Integration of epigenetic information with ASD genetic results may elucidate functional insights not possible via either source of information in isolation. We used concurrent genotype and DNA methylation (DNAm) data from cord blood and peripheral blood from preschool-aged children to identify SNPs associated with DNA methylation, or methylation quantitative trait loci (meQTLs), and combined this with publicly available fetal brain and lung meQTL lists to assess enrichment of ASD GWAS results for tissue-specific meQTLs. ASD-associated SNPs were enriched for fetal brain (OR = 3.55; $p < 0.001$) and peripheral blood meQTLs (OR = 1.58; $p < 0.001$). The CpG site targets of ASD meQTLs across cord, blood, and brain tissues were enriched for immune-related pathways, consistent with other expression and DNAm results in ASD, and revealing pathways not implicated by genes identified from ASD rare variant work. Further, DNaseI hypersensitive sites and the STAT1 and TAF1 transcription factor binding sites were enriched for meQTL target CpGs of SNPs associated with psychiatric conditions. This joint analysis of genotype and DNAm demonstrates the potential utility of both brain and blood-based DNAm for insights into ASD and psychiatric phenotypes more broadly.

bioRxiv preprint doi: https://doi.org/10.1101/091330; this version posted December 5, 2016. The copyright holder for this preprint (which was not certified by peer review) is the author/funder, who has granted bioRxiv a license to display the preprint in perpetuity. It is made available under aCC-BY 4.0 International license.

Autism spectrum disorder (ASD) is a complex neurodevelopmental disorder characterized by deficits in social communication and interaction, as well as restricted repetitive behavior[1], with a strong genetic basis[2,3]. Rare variants, including inherited and *de novo* mutations as well as copy number variations, are associated with ASD and related features[4–6]. Although rare variants explain a relatively small proportion of all ASD cases[7], they provide converging evidence for biological processes implicated in ASD[6,8,9]. Common genetic variation also plays a role, similar to other complex psychiatric diseases[10–12], and mega-analysis GWAS results from the Psychiatric Genomics Consortium ASD workgroup (PGC-AUT)[13], are currently available.

Previous studies of bipolar disorder[14], schizophrenia[15], and ASD[16] have demonstrated the enrichment of GWAS results for expression quantitative trait loci (eQTLs). Given the implications of epigenetic regulation in ASD from rare variant findings[6,8], the epigenetic basis of ASD-related conditions[17–19], and the association of histone modifications and DNA methylation in multiple tissues[20,21], similar examination of epigenetic marks is an important next step towards prioritization and characterization of ASD genetic results. As with expression loci, genetic variation contributes to DNAm levels locally and distally[22,23] and thus integration of methylation quantitative trait loci (meQTLs), or SNPs that are highly associated with DNAm, and autism-associated GWAS results may inform our understanding of autism GWAS findings. Moreover, meQTLs are enriched in top hits for bipolar disorder[14] and schizophrenia[15,22], which has a well-established genetic overlap with ASD[11].

Tissue specificity and corresponding accessibility are critical considerations for integration of meQTLs and ASD GWAS results. We and others have shown blood-based epigenetic biomarkers are useful in psychiatric conditions, including ASD[24,25], while recognizing the

bioRxiv preprint doi: https://doi.org/10.1101/091330; this version posted December 5, 2016. The copyright holder for this preprint (which was not certified by peer review) is the author/funder, who has granted bioRxiv a license to display the preprint in perpetuity. It is made available under aCC-BY 4.0 International license.

limitations and need for comparison to brain-derived data wherever possible[26–28]. ASD-related epigenetic differences have also been observed in buccal[29], lymphoblastoid cell line[30], and postmortem brain samples[31–33], as well as in the sperm from fathers of children with ASD[34]. Blood-brain concordance DNAm studies have not frequently observed high correlation of DNAm levels at specific sites across tissues, however, when such concordance is observed, it is likely due to genetic influences[26,27]. meQTL signals overlap in adult brain and blood tissues[35], suggesting blood-derived meQTLs may also reflect SNP-DNAm relationships in brain tissue, though this relationship has rarely been tested.

This study used meQTL maps from cord blood, peripheral blood, and fetal brain tissues to characterize and prioritize ASD GWAS SNPs and the CpG sites under their control. To achieve these goals, we: (1) identified meQTLs in infant cord and childhood peripheral blood tissues; (2) evaluated whether ASD GWAS signals are enriched for meQTLs from these tissues and fetal brain[22]; (3) identified CpG sites controlled by ASD-associated SNPs and the biological pathways enriched in these sites, and (4) demonstrated how consideration of the CpG sites controlled by ASD SNPs can implicate new genes not directly identified by GWAS results alone. We also sought to extend characterization of SNP-controlled CpG sites to neuropsychiatric disease more generally, through examination of overlap of these CpG sites with specific genomic regulatory features within and across tissue type. Our work demonstrates the utility of jointly analyzing GWAS and DNAm data for insights into ASD and neuropsychiatric disease.

RESULTS

Identifying meQTLs

bioRxiv preprint doi: https://doi.org/10.1101/091330; this version posted December 5, 2016. The copyright holder for this preprint (which was not certified by peer review) is the author/funder, who has granted bioRxiv a license to display the preprint in perpetuity. It is made available under aCC-BY 4.0 International license.

We identified meQTL SNPs using combined GWAS and 450K methylation array data available on both peripheral blood and cord blood samples. For these analyses, we defined study-specific parameters that were optimal for each dataset and determined the p-value to control the FDR at 10%, 5%, and 1%. In peripheral blood, we identified 1,878,577 meQTLs controlling DNAm at 85,250 CpGs; in cord blood, we found 1,252,498 meQTLs controlling DNAm at 35,905 CpGs, both at FDR = 5%. Peripheral blood and cord blood meQTLs, on average, were associated with 4.83 and 2.56 CpG sites respectively. Statistical significance was inversely related to distance between SNP and CpG site (**Supplementary Fig. 1**). We have provided a full list of all identified peripheral and cord blood meQTLs and their associated CpG sites at FDR = 5% (**Supplementary Data 1 and 2**).

We used publicly available lung[23] (to include a likely non ASD-related tissue) and fetal brain[22] meQTL lists and thus the p-value cutoffs stated in those respective studies (*P* = 1e-08 for fetal brain and *P* =4e-05 = FDR 5% for lung). In fetal brain, there were a total of 299,992 meQTLs controlling 7,863 CpGs, and in lung there were 22,866 meQTLs controlling 34,304 CpG sites. Dataset characteristics, meQTL parameters, and p-values used are summarized in **Table 1**.

There were 2,704,013 overlapping SNPs considered for meQTL discovery across peripheral blood, cord blood, and fetal brain analyses. Of these, 125,869 (4.65%) were identified as meQTLs in all three tissues, 407,722 (15.08%) were meQTLs only in peripheral and cord blood, 30,691 (1.14%) were meQTLs only in peripheral blood and fetal brain, and 528 (0.02%) were meQTLs only in cord blood and fetal brain (**Supplementary Table 1**).

bioRxiv preprint doi: https://doi.org/10.1101/091330; this version posted December 5, 2016. The copyright holder for this preprint (which was not certified by peer review) is the author/funder, who has granted bioRxiv a license to display the preprint in perpetuity. It is made available under aCC-BY 4.0 International license.

SNP-based test: Enrichment of meQTLs in ASD GWAS SNPs across 4 tissue types

We observed enrichment of fetal brain meQTLs at both the more liberal GWAS SNP p-value threshold (enrichment fold = 1.70, $P_{enrichment}$ < 1e-03, P_{GWAS} < 1e-03), and at a more GWAS p-value threshold (3.55, $P_{enrichment}$ < 1e-03, P_{GWAS} < 1e-04) (**Table 2**). There was no association with lung meQTLs at either the more liberal (1.09, $P_{enrichment}$ = 0.343) or more stringent (0.80, $P_{enrichment}$ = 0.301) threshold.

In peripheral and cord blood, we considered multiple GWAS SNP p-value thresholds as well as multiple meQTL discovery thresholds (the latter not available in brain and lung public data). There was significant meQTL enrichment for all GWAS and meQTL thresholds considered using peripheral blood meQTLs (enrichment fold range = 1.20 – 1.58, $P_{enrichment}$ < 1e-03; **Table 2**). However, in cord blood, meQTL enrichment was only observed for a liberal GWAS SNP threshold (range = 1.14 – 1.21, $P_{enrichment}$ = 0.011 – 0.032, P_{GWAS} < 1e-03). This was not statistically significant after considering a Bonferonni correction to account for the 16 enrichment tests performed.

CpG site-based test: Gene Ontology enrichment analyses of meQTL targets

We next examined the biological functions meQTL targets of ASD SNPs specifically compared to meQTL targets generally. We identified 210, 66, and 53 meQTL targets associated with ASD SNPs in peripheral blood, cord blood, and fetal brain respectively. After mapping these CpG sites to genes, performing GO enrichment analyses, and removing overlapping GO terms, there were a total 95, 76, and 47 nominally significant (p < 0.05) biological processes, respectively.

bioRxiv preprint doi: https://doi.org/10.1101/091330; this version posted December 5, 2016. The copyright holder for this preprint (which was not certified by peer review) is the author/funder, who has granted bioRxiv a license to display the preprint in perpetuity. It is made available under aCC-BY 4.0 International license.

A total of 37 biological processes were present across either two or three tissues (**Table 3, Supplementary Data 3-5**), many of them relating to immune system function. Of these, 3 terms overlapped across all three tissues, 12 processes were enriched in cord blood and fetal brain but not peripheral blood, and 22 processes were present in both the peripheral and cord blood but not in fetal brain.

To test whether our findings were unique to ASD meQTL targets, we performed the same analysis comparing all meQTL targets to all CpG sites. (**Supplementary Figs. 2-4**). Though there were some immune-related pathways discovered for fetal brain ASD meQTL targets that are also enriched in meQTLs generally, this was not the case in peripheral and cord blood.

Identifying novel genes or regions implicated by ASD meQTL target locations

The location of CpG targets for particular meQTL associations can further elucidate genes or regions relevant to ASD risk beyond the genomic location of the associated SNP variant. Of the 1,094 ASD-associated PGC SNPs (P < 1e-04), five (0.46%) were detected as meQTLs across peripheral blood, cord blood, and fetal brain tissues (**Supplementary Table 5, Supplementary Data 6**). Consideration of the CpG DNAm targets of these SNPs implicates genes not directly annotated to the SNPs themselves. For example, ASD SNPs in *XKR6* target CpGs in *TDH* in both peripheral blood and fetal brain, and target CpGs in *SOX7* peripheral blood and cord blood (**Fig. 1A**). A similar result can be seen for ASD SNPs in *PPFIA3* with meQTL target CpGs that implicate *HRC* (**Fig. 1B**).

bioRxiv preprint doi: https://doi.org/10.1101/091330; this version posted December 5, 2016. The copyright holder for this preprint (which was not certified by peer review) is the author/funder, who has granted bioRxiv a license to display the preprint in perpetuity. It is made available under aCC-BY 4.0 International license.

Regulatory features of meQTL targets within and across tissue type

We sought to quantify the propensity of regulatory features to overlap with meQTL targets within and across tissue type, and particularly whether meQTL targets of SNPs associated with psychiatric conditions have specific regulatory features. Individual and overlapping tissue meQTL target lists were compared for regulatory feature annotation. First, among psychiatric condition associated SNPs (via the PGC cross-disorder analysis[12]), their meQTL targets were significantly enriched for DNaseI hypersensitive sites (DHSs) in peripheral blood (OR = 1.22, P = 0.014), fetal brain (OR = 2.23, P = 3.5e-03), and peripheral blood-fetal brain overlap lists (OR = 2.22, P = 0.018; black font and boxes, **Fig. 2**), compared to meQTL targets of SNPs not associated with psychiatric conditions. Further, there was marginally significant enrichment of CD14 cell-specific DHSs (OR = 2.42, P = 0.013; **Supplementary Data 7**) in the peripheral blood-fetal brain list. Few chromatin marks met Bonferroni significance ($P \leq$ 3.95e-05) defined by the 181 tests of regulatory features performed in all 7 lists of meQTL targets, though numerous marginally significant enrichment associations were observed for blood H3K36me3 (active) and blood H3K27me3 (repressive). Transcription factor binding sites (TFBSs) with observed enrichment include (**Supplementary Data 7**) STAT1 for fetal brain (OR = 4.32, P = 2.66e-05) and peripheral blood (OR = 2.24, P = 3.56e-08), TAF1 for peripheral blood (OR = 1.53, P = 2.24e-06), cord blood (OR = 2.24, P = 4.01e-06), and fetal brain (OR = 3.2, P = 4.40e-06), and POL2RA for peripheral blood (OR = 1.38, P = 1.14e-06), cord blood (OR = 2.28, P = 3.54e-08), and their overlap (OR = 2.20, P = 9.63e-09).

When considering meQTL targets generally, compared to non-meQTL-target CpGs, enrichment was observed for DHSs for all 7 meQTL target lists, with the largest effect sizes among the

bioRxiv preprint doi: https://doi.org/10.1101/091330; this version posted December 5, 2016. The copyright holder for this preprint (which was not certified by peer review) is the author/funder, who has granted bioRxiv a license to display the preprint in perpetuity. It is made available under aCC-BY 4.0 International license.

peripheral blood-cord blood overlap list and the peripheral blood-fetal brain overlap list (gray font and boxes, **Fig. 2**). This relationship is less clear when considering cell type-specific DHSs; though we do observe consistent enrichment in the same overlap lists (**Supplementary Data 8**). Significant feature enrichment (OR > 1, $p < 3.95x10^{-5}$) of meQTL targets in the overlapping peripheral blood and fetal brain list highlights a functional role in both activating (H3K4me1, H3K4me3) and repressing (H3K27me3, H3K9me3) histone marks. Also, enrichment of TFBSs (SETDB1, CTCF, PLR2A, RAD21, MAX, and SMC3) was higher in the peripheral blood and fetal brain overlap meQTL list compared to either tissue individually (**Supplementary Data 8**). Many of these same features showed enrichment in lung tissue as well.

DISCUSSION

We provide the first study integrating ASD GWAS results and meQTL data that provide novel insights towards ASD etiology using data within and across tissue types. First, using blood samples from birth and early life, we identified meQTLs and compared them to previously reported fetal brain tissue meQTLs and found a subset of SNPs that were detected as meQTLs across all three tissues. However, the highest percent overlap was seen across peripheral and cord blood only, which is expected given their tissue similarity. Second, we observed enrichment of peripheral blood ($1.20 \leq OR \leq 1.58$; $p < 0.001$) and fetal brain (OR = 1.70 and 3.55; $p < 0.001$) meQTLs among PGC-AUT mega-analysis findings. Third, when considering the biological processes annotated to ASD meQTL targets, we found enrichment for immune-related pathways in all three tissues. Fourth, we show how meQTL targets may suggest novel regions for functional follow-up ASD genetic associations. Finally, we identified several regulatory elements that preferentially overlap with meQTL targets associated with known SNPs for

bioRxiv preprint doi: https://doi.org/10.1101/091330; this version posted December 5, 2016. The copyright holder for this preprint (which was not certified by peer review) is the author/funder, who has granted bioRxiv a license to display the preprint in perpetuity. It is made available under aCC-BY 4.0 International license.

neuropsychiatric disease generally. Our results demonstrate the utility of meQTLs and their CpG targets for insights into ASD and neuropsychiatric disease overall.

We compared meQTL lists across tissues, which presents several challenges to consider when interpreting results. First, each set of samples came from a different study source, reflecting different sets of individuals and different sampling strategies, as well as differences in sample size and in genotyping and methylation array platforms. For example, we expected and observed considerable overlap between cord and peripheral blood meQTL signals, and less overlap with brain, however the lack of further cross-tissue concordance with brain could be due to limited statistical power between studies, lack of SNP or CpG overlap on arrays or post QC, or differences in meQTL discovery association parameters (window size, SNP MAF, etc.). In our functional characterization of meQTL targets, we used down sampling of peripheral blood results to the sample size and meQTL query parameters of the tissue to which it was being compared. While this is likely an incomplete solution, it is a step toward harmonization that has not been carried out in other studies.

We demonstrate that joint analysis of SNP and DNAm data can reveal novel insights towards ASD etiology not apparent when looking at either type of data alone. It is important to examine the biological implications of the genes implicated by SNPs, as well as the genes and regulatory functions implicated by DNAm. When considering the ASD SNPs, we found enrichment of fetal brain and peripheral blood meQTLs that was robust to both meQTL p-value threshold and ASD p-value threshold. These results are concordant with similar studies of schizophrenia, a disorder

bioRxiv preprint doi: https://doi.org/10.1101/091330; this version posted December 5, 2016. The copyright holder for this preprint (which was not certified by peer review) is the author/funder, who has granted bioRxiv a license to display the preprint in perpetuity. It is made available under aCC-BY 4.0 International license.

with known genetic overlap to ASD[11], that have demonstrated enrichment in fetal brain meQTLs[22] and peripheral blood meQTLs[15]. A previous study examining enrichment of eQTLs in ASD GWAS SNPs observed enrichment in parietal and cerebellar eQTLs but not lymphoblastoid cell line eQTLs[16], though the GWAS results in that report likely differ greatly from those of the larger PGC-AUT mega-analysis. Crucially, we did not observe enrichment of lung meQTLs, supporting the specificity of fetal brain and peripheral blood results. However, we also did not observe an enrichment of cord blood meQTLs, suggesting the role of ASD-related DNAm marks in peripheral tissues may be developmentally regulated or a function of age. Additional insights may be gained through examination of specific CpG targets of the ASD-related SNPs. As discussed below, examination of processes implicated by CpG targets of ASD SNPs highlights immune function. It is plausible that environmental experience in early (postnatal) life is critical in contributing to DNAm variability that enables the detection of blood meQTLs and that cord blood does not yet reflect that interplay.

Among CpG sites that are targets of ASD SNP meQTLs, there is an abundance of immune response-related pathways, using brain, peripheral blood, or cord blood meQTL lists. This immune enrichment was not seen when considering CpG targets of all meQTLs in blood (not just the ASD SNPs), suggesting specificity to ASD. However, such enrichment was seen for all meQTL targets in fetal brain. This may be a consequence of the complications during pregnancy that resulted in fetal tissue collection (56-166 days post conception[22]). Though many immune-related disorders are known to be comorbid with ASD[36], previous enrichment-type analysis for genetic variants alone have not highlighted immune-related pathways, instead implicating chromatin regulation, synaptic function, and Wnt signaling[6,9], particularly for genes implicated

bioRxiv preprint doi: https://doi.org/10.1101/091330; this version posted December 5, 2016. The copyright holder for this preprint (which was not certified by peer review) is the author/funder, who has granted bioRxiv a license to display the preprint in perpetuity. It is made available under aCC-BY 4.0 International license.

via rare variants. However, several gene expression and epigenetic studies of ASD have implicated immune function in both brain tissue[31,37–39] and peripheral blood[40,41]. Our results are concordant with these expression and epigenetic studies but still suggest a role for genetic variation in contributing to immune dysregulation in ASD, through SNP control of DNAm.

Beyond genome and epigenome enrichment analyses, specific meQTL targets also helped to "expand" ASD GWAS-implicated regions to include CpG sites, and their associated genes. While this does not increase or decrease statistical support for a particular GWAS SNP finding, better characterization of the functional architecture of the region can inform follow-up analyses of these hits. Two GWAS loci displayed evidence of meQTLs in peripheral blood, cord blood, and fetal brain, and many more loci displayed evidence of meQTLs in at least one tissue. These target CpG sites, and the genes they implicate, would not be identified via traditional genetic (i.e. GWAS) analyses, since the sequence itself does not show ASD-related variability in these areas. Insights emerge only through the integration of SNP and DNAm data. Current PGC-AUT GWAS results are likely underpowered to provide reliable genome-wide hits. As larger GWAS of ASD emerge with higher-confidence findings, this cross-tissue meQTL mapping approach should be used to expand regions for follow-up, as recently demonstrated for schizophrenia in fetal brain [22].

Finally, we sought to understand the propensity of meQTL targets, both generally and those controlled by psychiatric disorder-related SNPs, to overlap with regions of known functional activity. MeQTL targets of psychiatric SNPs in peripheral blood, fetal brain, and their intersection significantly overlapped with DHS sites, a result that is concordant with our

bioRxiv preprint doi: https://doi.org/10.1101/091330; this version posted December 5, 2016. The copyright holder for this preprint (which was not certified by peer review) is the author/funder, who has granted bioRxiv a license to display the preprint in perpetuity. It is made available under aCC-BY 4.0 International license.

observation of meQTL enrichment among ASD SNPs limited to peripheral blood and fetal brain. We also identified specific TFBSs enriched in psychiatric disorder meQTL targets such as TAF1 and STAT1. Recently, a study of nine families demonstrated both *de novo* and maternally inherited single nucleotide changes in *TAF1* to be associated with intellectual disability, facial dysmorphology, and neurological manifestations[42]. Our finding that binding sites for the TAF1 transcription factor overlap meQTL targets of psychiatric SNPs could serve a basis for future functional studies examining the link between *TAF1* mutations and adverse neurological phenotypes. Lastly, mutations in *STAT1* have been linked to early life combined immunodeficiency[43]. The significant overlap with STAT1 TFBSs could thus serve as a starting point for functional work looking to understand the role of immune disorders in ASD and psychiatric phenotypes generally.

In summary, our work is the first genome-wide study of meQTLs in the context of ASD to date. The results point to the utility of both brain and blood tissues in studies of ASD that integrate epigenetic data to enhance current GWAS findings for ASD. We show the utility of examining the meQTL targets of ASD SNPs in providing novel insights into functional roles like immune system processes that would not be apparent via genotype-based analysis in isolation. Our work suggests that genetic and epigenetic data integration, from a variety of tissues, will continue to provide ASD-related functional insights as GWAS findings and meQTL mapping across a variety of tissues improve.

METHODS

bioRxiv preprint doi: https://doi.org/10.1101/091330; this version posted December 5, 2016. The copyright holder for this preprint (which was not certified by peer review) is the author/funder, who has granted bioRxiv a license to display the preprint in perpetuity. It is made available under aCC-BY 4.0 International license.

Cord blood samples

Cord blood DNA was obtained from newborn participants of the Early Autism Risk Longitudinal Risk Investigation (EARLI), an enriched-risk prospective birth cohort described in detail elsewhere[44]. The EARLI study was approved by Human Subjects Institutional Review Boards (IRBs) from each of the four study sites (Johns Hopkins University, Drexel University, University of California Davis, and Kaiser Permanente). Mothers of confirmed ASD children were recruited during a subsequent pregnancy. The 232 mothers with a subsequent sibling born through this study had births between November 2009 and March 2012. Infants were followed with extensive neurophenotyping until age three, including ASD diagnostics.

Cord blood DNA methylation

Cord blood biospecimens were collected and archived at 175 births. DNA was extracted using the DNA Midi kit (Qiagen, Valencia, CA) and samples were bisulfite treated and cleaned using the EZ DNA methylation gold kit (Zymo Research, Irvine, CA). DNA was plated randomly and assayed on the Infinium HumanMethylation450 BeadChip (Illumina, San Diego, CA), or "450k", at the Center for Inherited Disease Research (CIDR, Johns Hopkins University). Methylation control gradients and between-plate repeated tissue controls (n=68) were used[34]. The *minfi* library (version 1.12)[45] in R (version 3.1) was used to process raw Illumina image files with the background correcting and dye-bias equalization method: normal-exponential using out-of-band probe (Noob)[46,47]. Probes with failed detection P-value (>0.01) in >10% of samples were removed (n=661), as were probes annotated as cross-reactive (n=29,233)[48] and those mapping to sex chromosomes (n=11,648). All cord samples passed sample-based filters (sex matching, detection p-values > 0.01 in greater than 1% of sites). Pre-processed data were adjusted for batch

bioRxiv preprint doi: https://doi.org/10.1101/091330; this version posted December 5, 2016. The copyright holder for this preprint (which was not certified by peer review) is the author/funder, who has granted bioRxiv a license to display the preprint in perpetuity. It is made available under aCC-BY 4.0 International license.

effects related to hybridization date and array position using the *ComBat()* function[49] in the *sva* R package (version 3.9.1)[50]. Methylation data were available from 175 cord blood samples at 445,241 probes.

Cord blood genotyping

Overlapping cord blood DNA methylation and corresponding SNP data was available on 171 EARLI cord blood samples. Genotype data were generated for 841 EARLI family biosamples and 18 HapMap control samples run on the Omni5 plus exome (Illumina, San Diego, CA) genotyping array at CIDR (Johns Hopkins University), generating data on 4,641,218 SNPs. The duplicated HapMap sample concordance rate was 99.72% and the concordance rate among five EARLI samples with blind duplicates was 99.9%. Samples were removed if they were HapMap controls (n=18), technical duplicates (n=5; selected by frequency of missing genotypes), or re-enrolled families/other relatedness errors (n=9). No samples met the following additional criteria for exclusion: missing genotypes at >3% of probes, or excess heterozygosity or homozygosity (4 SD). Probes were removed for CIDR technical problems (n=94,712), missing genomic location information (n=8,124). Among probes with high minor allele frequencies (>5%), SNPs with a missing rate $\geq$ 5% were excluded (n=8,902) and among probes with low minor allele frequencies (<5%) SNPs with a missing rate >1% were excluded (n=65,855). There were 827 samples and 4,463,625 probes at this stage and SNPs out of Hardy-Weinberg equilibrium (p<10-7) were flagged (n=2,170). Samples were merged with the 1,000 genomes project (1000GP, version 5) data[51] and EARLI ancestries were projected into four categories (White, Black, Asian, Hispanic). EARLI measured genotype data was phased using SHAPEIT[52] and imputed to the 1000GP data using Minimac3[53]. SNPs with MAF > 1% were retained, leaving a total of 9,377,008 SNPs.

bioRxiv preprint doi: https://doi.org/10.1101/091330; this version posted December 5, 2016. The copyright holder for this preprint (which was not certified by peer review) is the author/funder, who has granted bioRxiv a license to display the preprint in perpetuity. It is made available under aCC-BY 4.0 International license.

Peripheral blood samples

Samples were obtained from the Study to Explore Early Development (SEED), a multi-site, national case-control study of children aged 3-5 years with and without ASD. Overall, 2,800 families were recruited and classified into 3 groups according to the status of the child: the ASD group, the general population control group, and the (non-ASD) developmental delay group[54]. This study was approved as an exemption from the Johns Hopkins Institutional Review Board (IRB) under approval 00000011. Informed consent was obtained from all participants as part of the parent SEED study. SEED recruitment was approved by the IRBs of each recruitment site: Institutional Review Board (IRB)-C, CDC Human Research Protection Office; Kaiser Foundation Research Institute (KFRI) Kaiser Permanente Northern California IRB, Colorado Multiple IRB, Emory University IRB, Georgia Department of Public Health IRB, Maryland Department of Health and Mental Hygiene IRB, Johns Hopkins Bloomberg School of Public Health Review Board, University of North Carolina IRB and Office of Human Research Ethics, IRB of The Children's Hospital of Philadelphia, and IRB of the University of Pennsylvania. All enrolled families provided written consent for participation.

Peripheral blood DNA methylation

Genomic DNA was isolated from whole blood samples using the QIAsumphonia midi kit (Qiagen, Valencia, CA). For each a subset of case and control samples (n = 630), bisulfite treatment was performed using the 96-well EZ DNA methylation kit (Zymo Research, Irvine, CA). Samples were randomized within and across plates to minimize batch and position effects. The minfi R package (version 1.16.1) was used to process Illumina .idat files generated from the

bioRxiv preprint doi: https://doi.org/10.1101/091330; this version posted December 5, 2016. The copyright holder for this preprint (which was not certified by peer review) is the author/funder, who has granted bioRxiv a license to display the preprint in perpetuity. It is made available under aCC-BY 4.0 International license.

array[45]. Control samples (n=14) were removed and quantile normalization performed using the *minfi* function *preprocessQuantile()*[55]. Probes with failed detection P-value (>0.01) in >10% of samples were removed (n=772), as were probes annotated as cross-reactive (n=29,233)[48], and probes on sex chromosomes (n=11,648). Samples were excluded if reported sex did not match predicted sex (*minfi* function *getSex()*) (n=0), detection p-values > 0.01 in greater than 1% of sites (n=2), low overall intensity (median methylated or unmethylated intensity < 11; n=2), and if they were duplicates (n=8). Successive filtering according to these criteria resulted in 445,154 probes and 604 samples.

Peripheral blood genotyping

Of the SEED samples with DNAm data, 590 had whole-genome genotyping data available, measured using the Illumina HumanOmni1-Quad BeadChip (Illumina, San Diego, CA). Standard quality control measures were applied: removing samples with < 95% SNP call rate, sex discrepancies, relatedness (Pi-hat > 0.2), or excess hetero- or homozygosity; removing markers with < 98.5% call rate, or monomorphic. Phasing was performed using SHAPEIT[52] followed by SNP imputation via the IMPUTE2 software[53], with all individuals in the 1000 Genomes Project as a reference. Genetic ancestry was determined using EigenStrat program[56]. A total of 4,948,723 SNPs were available post imputation at MAF > 1%.

Normal lung tissue meQTLs

A list of meQTLs identified in a recent characterization of normal lung tissue[23] as well as the total list of SNPs (n = 569,753) and 450k CpG sites (n = 338,730) tested for meQTL identification (i.e. passed filtering and QC done in that study) was obtained from the study authors.

bioRxiv preprint doi: https://doi.org/10.1101/091330; this version posted December 5, 2016. The copyright holder for this preprint (which was not certified by peer review) is the author/funder, who has granted bioRxiv a license to display the preprint in perpetuity. It is made available under aCC-BY 4.0 International license.

Fetal brain meQTLs

Fetal brain meQTLs were identified via imputed genotypes in a recent study examining meQTLs in the context of schizophrenia[22]. The total list of SNPs (n = 5,159,699) and 450k CpG sites (n = 314,554) that were tested (i.e. passed filtering and QC done in that study) was obtained from the study authors. For all analyses, only fetal brain meQTLs within a SNP to CpG distance of 1 Mb, were included, in order to improve comparability to the other 3 meQTL lists, where distant (trans) meQTL relationships were not explored (peripheral blood, cord blood) or used (lung).

meQTL identification parameters

There are three main parameters of interest in a meQTL query: the SNP minor allele frequency (MAF) threshold for inclusion, the definition of standard deviation cutoff that dictates a CpG site is variably methylated, and the maximum physical distance between a SNP and CpG site to be queried, often referred to as the window size. These 3 factors contribute to the total number of CpG to SNP linear regression tests that are performed. Our available sample sizes (and thus statistical power, at fixed effect size) for the joint DNAm and genotype data differed for peripheral blood and cord blood analyses. Thus, the ideal combination of these parameters should differ between the two study populations to be comparable.

For each tissue sample set, we computed the total number of CpG to SNP linear regression tests at various combinations of the 3 main parameters of interest to a meQTL query. We then used the genetic power calculator Quanto[57] to determine the most permissive set of parameters that allowed for 80% power to detect a 5% difference in methylation for each addition of the minor allele, at the lowest allowed MAF. We computed this power calculation at a Bonferroni-based significance level derived from the total number of CpG to SNP linear regression tests. We

bioRxiv preprint doi: https://doi.org/10.1101/091330; this version posted December 5, 2016. The copyright holder for this preprint (which was not certified by peer review) is the author/funder, who has granted bioRxiv a license to display the preprint in perpetuity. It is made available under aCC-BY 4.0 International license.

defined 'most permissive' in a hierarchical manner that first prioritized the inclusion of the most methylation sites (lowest sd cutoff), then the inclusion of the most number of SNPs (lowest MAF threshold), and then the use of the largest window size. This procedure resulted in study-specific MAF thresholds for the SNP data, standard deviation cutoffs for the methylation data, and window sizes that were tailored to the number of samples available.

meQTL identification procedure

Pairwise associations between each SNP and CpG site were estimated via the R package *MatrixEQTL*[58], with percent methylation (termed 'Beta value', ranging from 0 to 100) regressed onto genotype assuming an additive model, adjusting for the first two principal components of ancestry and sex. Models did not adjust for age given the very narrow age ranges in each tissue type.

False discovery rate (FDR) was controlled via permutation[23]. Briefly, the total number of CpG sites (N_{obs}) under genetic control was obtained for a meQTL p-value of p_o. Genome-wide meQTL query was performed for each of 100 permuted sets of the genotype data (scrambling sample IDs, to retain genotype correlation structure). In each set, we retained the total number of CpG sites under genetic control (N_{null}) at the same p-value p_o. The FDR was defined as the mean(N_{null})/ N_{obs}. Finally we determined the value of p_o to control the FDR at values of 10%, 5%, and 1%. Both the meQTL discovery and FDR determination were performed in each tissue or study sample.

Enrichment of meQTLs in ASD-associated SNPs

bioRxiv preprint doi: https://doi.org/10.1101/091330; this version posted December 5, 2016. The copyright holder for this preprint (which was not certified by peer review) is the author/funder, who has granted bioRxiv a license to display the preprint in perpetuity. It is made available under aCC-BY 4.0 International license.

We tested for enrichment of meQTLs from four tissue types among ASD GWAS SNPs. ASD SNPs were assigned from the PGC-AUT analysis (downloaded February 2016), based on 5,305 cases and 5,305 pseudocontrols[13,59]. For each tissue, we included only SNPs available in both the PGC-AUT analysis and our meQTL analysis, either via direct or proxy ($r^2 > 0.8$ within 500Kb window in CEU 1KG) overlap as defined via the SNAP software[60].

To estimate the proportion of meQTLs among ASD SNPs versus among all SNPs (or a sample of null SNPs), we recognized three important factors that could differ between null SNP sets and the ASD SNP set: LD structure, MAF distribution, and number of CpG sites per window size in the meQTL screen. We designed a comparison process to address each of these. First, we performed LD pruning 'supervised' by PGC ASD p-value (so as to not prune away all ASD SNPs) using PriorityPruner (v0.1.2)[61], removing SNPs at $r^2 > 0.7$ within a sliding 500Kb window. For the peripheral blood and cord blood datasets this pruning was done with the study-specific genotype data, and for the fetal brain and lung datasets this pruning was done with 1000 Genomes CEU samples. Second, we grouped remaining SNPs into MAF bins of 5%. Third, we characterized each SNP according to the number of CpGs within the meQTL discovery window size to allow for differential opportunity to have been identified as a meQTL. We then collapsed this number into categories of 0-49, 50-99, etc. to reflect the same concept. We defined 1,000 null SNP sets by finding, for each SNP in the ASD set, a random SNP in the genome that matched that SNP on both MAF bin and CpG opportunity. We computed an enrichment fold statistic as the proportion of meQTLs in the ASD SNP set divided by the mean proportion of meQTLs across null sets; and a p-value as the total number of null set proportions as or more extreme than in the ASD set. To evaluate the robustness of our results, we used two PGC AUT

bioRxiv preprint doi: https://doi.org/10.1101/091330; this version posted December 5, 2016. The copyright holder for this preprint (which was not certified by peer review) is the author/funder, who has granted bioRxiv a license to display the preprint in perpetuity. It is made available under aCC-BY 4.0 International license.

p-value cutoffs (1e-03, 1e-04) and three meQTL p-value cutoffs (FDR 10%, 5%, 1%) for peripheral blood and cord blood. However, based on available information for lung and fetal brain, we were limited to assess our results at FDR 5% for lung, and p<1e-08 for fetal brain for meQTL p-value.

Gene ontology analysis of meQTL targets

We identified Gene Ontology (GO) terms specific to CpG sites associated with ASD SNPs (ASD-related meQTL targets) compared to those associated with CpG sites controlled by SNPs generally (all meQTL targets) in order to enumerate biological pathways engaged specifically by ASD SNPs. We first filtered the full list of CpG sites associated with any meQTL to only those sites associated with an ASD SNP (PGC P < 1e-04; N=1,094) or their proxies (r^2 > 0.8 within 500kb window in CEU 1KG as defined via the SNAP software[60]). We used thresholds of FDR ≤ 5% for peripheral and cord blood meQTL lists, and P < 1e-08 for the fetal brain list. We only examined CpG sites that did not overlap with SNPs within 10bp of the CpG site or at the single base extension[62], as it has been previously demonstrated that these CpG sites may strongly influence functional-type enrichment analysis of CpG sites[63], and these CpG sites were not examined in the fetal brain meQTL lists[22]. We used the *gometh()* function in the *MissMethyl* R package[64], which maps 450k DNAm sites to their nearest gene, and corrects for bias due to non-uniform coverage of genes on the 450k. We further ran nominally significant (p < 0.05) results for the category "biological processes" through the REVIGO tool to avoid reporting GO terms with a greater than 70% overlap in gene lists[65]. Finally, we determined the set of terms in these lists that overlapped at least two tissues, and prioritized them by summing the scaled, enrichment p-value-based rank in each tissue. This scaling was done by dividing the raw rank for the term in

bioRxiv preprint doi: https://doi.org/10.1101/091330; this version posted December 5, 2016. The copyright holder for this preprint (which was not certified by peer review) is the author/funder, who has granted bioRxiv a license to display the preprint in perpetuity. It is made available under aCC-BY 4.0 International license.

the list for that tissue by the total number of nominally significant, post-REVIGO terms for that tissue.

We also ran analogous GO analyses comparing all meQTL targets to all CpGs to explore functional implications for meQTL targets versus CpGs not under strong genetic control. This allowed for comparison of ASD SNP-specific functional pathways engaged through methylation versus general SNP functional pathways engaged through methylation.

Identifying novel genes or regions implicated by ASD meQTL target locations

Defining ASD SNPs as those with PGC p-value < 1e-04, meQTL relationships as in the GO analysis, and RefSeq genes from the UCSC Genome Browser[66], we annotated gene overlap (if any) via *findOverlaps()* in the *GenomicRanges* R package for all ASD SNPs and their associated CpG sites (if any). We filtered out long intergenic non-coding RNAs, long non-coding RNAs, microRNAs, and small associated RNAs from the RefSeq gene list. We further collapsed SNPs into bins by LD block. Blocks were defined using recombination hot spot data from 1000 Genomes[51].

Regulatory feature characterization of meQTL targets

To quantify the propensity of regulatory features to overlap with meQTL targets within and across tissue type, we first compared regulatory feature overlap of all meQTL targets to non-meQTL targets. We next compared meQTL targets of psychiatric condition-related SNPs to meQTL targets of SNPs unrelated to psychiatric conditions. SNPs associated with psychiatric conditions were obtained from the PGC cross-disorder analysis[12] (PGC P < 1e-04) and their proxies. We used these SNPs in order to analyze a greater total number of meQTL targets than

bioRxiv preprint doi: https://doi.org/10.1101/091330; this version posted December 5, 2016. The copyright holder for this preprint (which was not certified by peer review) is the author/funder, who has granted bioRxiv a license to display the preprint in perpetuity. It is made available under aCC-BY 4.0 International license.

associated with ASD SNPs only, and to make functional insights that could be applied to psychiatric disease more broadly.

We performed both comparisons for unique and overlapping tissue categories (n =7): peripheral blood, cord blood, fetal brain, lung, intersection of peripheral blood and cord blood, intersection of peripheral blood and fetal brain, and intersection of peripheral blood and lung. For each intersection, we conducted a new meQTL discovery screen in which the peripheral blood was down sampled to the sample size of the other tissue, and run at the same parameters used to identify meQTLs in that tissue. This increases comparability with respect to power and meQTL query parameters. For the peripheral blood overlaps with cord blood and lung, we also computed the meQTL p-value to control the FDR at 5% using the method previously described, as this parameter value was available for those tissue sample meQTL results[23]. However, we only computed the FDR p-values using data from the first 6 chromosomes, as we found empirically that FDR p-value estimates stabilized by this point. Finally, for the peripheral blood-fetal brain comparison, we retained results for peripheral blood that passed a meQTL p-value of 1E-8, as reported from the fetal brain study[22].

Regulatory feature information came from several sources. General DHSs were defined as those CpG probes experimentally determined to be within a DHS, as determined by the manifest for the 450k array[67]. In addition, tissue-specific DHS data were tested for enrichment. Brain DHSs were downloaded in from GEO[68] for three brain regions: Frontal Cortex [GEO Sample ID: GSM1008566], Cerebellum [GSM1008583], and Cerebrum [GSM1008578]). Two blood (CD14+ Monocytes; ‘wgEncodeOpenChromDnaseMonocd14’ and CD4+ cells; ‘wgEncodeUwDnaseCd4naivewb78495824PkRep1’) and one lung-derived (IMR90;

bioRxiv preprint doi: https://doi.org/10.1101/091330; this version posted December 5, 2016. The copyright holder for this preprint (which was not certified by peer review) is the author/funder, who has granted bioRxiv a license to display the preprint in perpetuity. It is made available under aCC-BY 4.0 International license.

'wgEncodeOpenChromDnaseImr90Pk') data sets were additionally downloaded from the UCSC Genome Browser[66].

Tissue-specific histone data were compiled from the Roadmap Epigenomics Project[69] for five different marks: H3K27me3, H3K36me3, H3K4me1, H3K4me3, and H3K9me3. As Epigenome Roadmap Project data were often generated across a number of individuals, for those cases in which data were generated in more than one Caucasian individual, the overlap across individual samples was utilized in downstream analyses. Overlap was calculated using the UCSC Genome Browser's '*intersect*' function for those samples indicated in **Table 4**. Regions with any overlap were included in functional enrichment analyses.

Table 4: Samples downloaded from Roadmap Epigenomics Project for 5 different histone modifications.

	H3K27me3	**H3K36me3**	**H3K4me1**	**H3K4me3**	**H3K9me3**
Adult Lung	NA	GSM1059437	GSM1059443	GSM1227065	GSM1120355
	GSM1220283	GSM956014	GSM910572	GSM915336	GSM906411
Fetal Brain	GSM621393	GSM621410	GSM706850	GSM621457	GSM621427
	GSM916061				GSM916054
Peripheral Blood	GSM1127130	GSM1127131	GSM1127143	GSM1127126	GSM1127133
	GSM1127142	GSM613880			GSM613878

Finally, TFBS information from ChIP-Seq experiments carried out by the ENCODE project[70] were extracted for 161 transcription factors from the UCSC Genome Browser ('wgEncodeRegTfbsClusteredV3')[66].

bioRxiv preprint doi: https://doi.org/10.1101/091330; this version posted December 5, 2016. The copyright holder for this preprint (which was not certified by peer review) is the author/funder, who has granted bioRxiv a license to display the preprint in perpetuity. It is made available under aCC-BY 4.0 International license.

Significant feature overlap was assessed via two-sided Fisher's 2x2 exact test, with Bonferroni correction ($p < 0.05$ / (181 regulatory features * 7 categories) = 3.95e-05). Odds ratio and p-value were recorded for each test in each unique and overlapping tissue category.

REFERENCES

1. Rapin, I. Autism. *N. Engl. J. Med.* **337,** 97–104 (1997).
2. Sandin, S. *et al.* The familial risk of autism. *JAMA* **311,** 1770–1777 (2014).
3. Colvert, E. *et al.* Heritability of Autism Spectrum Disorder in a UK Population-Based Twin Sample. *JAMA Psychiatry* **72,** 415–423 (2015).
4. Iossifov, I. *et al.* The contribution of de novo coding mutations to autism spectrum disorder. *Nature* **515,** 216–221 (2014).
5. O'Roak, B. J. *et al.* Recurrent de novo mutations implicate novel genes underlying simplex autism risk. *Nat. Commun.* **5,** 5595 (2014).
6. Sanders, S. J. *et al.* Insights into Autism Spectrum Disorder Genomic Architecture and Biology from 71 Risk Loci. *Neuron* **87,** 1215–1233 (2015).
7. Gaugler, T. *et al.* Most genetic risk for autism resides with common variation. *Nat. Genet.* **46,** 881–885 (2014).
8. Pinto, D. *et al.* Convergence of genes and cellular pathways dysregulated in autism spectrum disorders. *Am. J. Hum. Genet.* **94,** 677–694 (2014).
9. Krumm, N., O'Roak, B. J., Shendure, J. & Eichler, E. E. A de novo convergence of autism genetics and molecular neuroscience. *Trends Neurosci.* **37,** 95–105 (2014).
10. Schizophrenia Working Group of the Psychiatric Genomics Consortium. Biological insights from 108 schizophrenia-associated genetic loci. *Nature* **511,** 421–427 (2014).

bioRxiv preprint doi: https://doi.org/10.1101/091330; this version posted December 5, 2016. The copyright holder for this preprint (which was not certified by peer review) is the author/funder, who has granted bioRxiv a license to display the preprint in perpetuity. It is made available under aCC-BY 4.0 International license.

11. Cross-Disorder Group of the Psychiatric Genomics Consortium *et al.* Genetic relationship between five psychiatric disorders estimated from genome-wide SNPs. *Nat. Genet.* **45,** 984–994 (2013).

12. Cross-Disorder Group of the Psychiatric Genomics Consortium. Identification of risk loci with shared effects on five major psychiatric disorders: a genome-wide analysis. *Lancet Lond. Engl.* **381,** 1371–1379 (2013).

13. Psychiatric Genomics Consortium. Available at: http://www.med.unc.edu/pgc. (Accessed: 5th August 2016)

14. Gamazon, E. R. *et al.* Enrichment of cis-regulatory gene expression SNPs and methylation quantitative trait loci among bipolar disorder susceptibility variants. *Mol. Psychiatry* **18,** 340–346 (2013).

15. van Eijk, K. R. *et al.* Identification of schizophrenia-associated loci by combining DNA methylation and gene expression data from whole blood. *Eur. J. Hum. Genet. EJHG* **23,** 1106–1110 (2015).

16. Davis, L. K. *et al.* Loci nominally associated with autism from genome-wide analysis show enrichment of brain expression quantitative trait loci but not lymphoblastoid cell line expression quantitative trait loci. *Mol. Autism* **3,** 3 (2012).

17. Horsthemke, B. & Wagstaff, J. Mechanisms of imprinting of the Prader-Willi/Angelman region. *Am. J. Med. Genet. A.* **146A,** 2041–2052 (2008).

18. Amir, R. E. *et al.* Rett syndrome is caused by mutations in X-linked MECP2, encoding methyl-CpG-binding protein 2. *Nat. Genet.* **23,** 185–188 (1999).

bioRxiv preprint doi: https://doi.org/10.1101/091330; this version posted December 5, 2016. The copyright holder for this preprint (which was not certified by peer review) is the author/funder, who has granted bioRxiv a license to display the preprint in perpetuity. It is made available under aCC-BY 4.0 International license.

19. Oberlé, I. *et al.* Instability of a 550-base pair DNA segment and abnormal methylation in fragile X syndrome. *Science* **252,** 1097–1102 (1991).

20. Loke, Y. J., Hannan, A. J. & Craig, J. M. The Role of Epigenetic Change in Autism Spectrum Disorders. *Front. Neurol.* **6,** 107 (2015).

21. Abdolmaleky, H. M., Zhou, J.-R. & Thiagalingam, S. An update on the epigenetics of psychotic diseases and autism. *Epigenomics* **7,** 427–449 (2015).

22. Hannon, E. *et al.* Methylation QTLs in the developing brain and their enrichment in schizophrenia risk loci. *Nat. Neurosci.* **19,** 48–54 (2016).

23. Shi, J. *et al.* Characterizing the genetic basis of methylome diversity in histologically normal human lung tissue. *Nat. Commun.* **5,** 3365 (2014).

24. Wong, C. C. Y. *et al.* Methylomic analysis of monozygotic twins discordant for autism spectrum disorder and related behavioural traits. *Mol. Psychiatry* **19,** 495–503 (2014).

25. Montano, C. *et al.* Association of DNA Methylation Differences With Schizophrenia in an Epigenome-Wide Association Study. *JAMA Psychiatry* **73,** 506–514 (2016).

26. Davies, M. N. *et al.* Functional annotation of the human brain methylome identifies tissue-specific epigenetic variation across brain and blood. *Genome Biol.* **13,** R43 (2012).

27. Hannon, E., Lunnon, K., Schalkwyk, L. & Mill, J. Interindividual methylomic variation across blood, cortex, and cerebellum: implications for epigenetic studies of neurological and neuropsychiatric phenotypes. *Epigenetics* **10,** 1024–1032 (2015).

28. Bakulski, K. M., Halladay, A., Hu, V. W., Mill, J. & Fallin, M. D. Epigenetic Research in Neuropsychiatric Disorders: the 'Tissue Issue'. *Curr. Behav. Neurosci. Rep.* **3,** 264–274 (2016).

bioRxiv preprint doi: https://doi.org/10.1101/091330; this version posted December 5, 2016. The copyright holder for this preprint (which was not certified by peer review) is the author/funder, who has granted bioRxiv a license to display the preprint in perpetuity. It is made available under aCC-BY 4.0 International license.

29. Berko, E. R. *et al.* Mosaic epigenetic dysregulation of ectodermal cells in autism spectrum disorder. *PLoS Genet.* **10,** e1004402 (2014).

30. Nguyen, A., Rauch, T. A., Pfeifer, G. P. & Hu, V. W. Global methylation profiling of lymphoblastoid cell lines reveals epigenetic contributions to autism spectrum disorders and a novel autism candidate gene, RORA, whose protein product is reduced in autistic brain. *FASEB J. Off. Publ. Fed. Am. Soc. Exp. Biol.* **24,** 3036–3051 (2010).

31. Nardone, S. *et al.* DNA methylation analysis of the autistic brain reveals multiple dysregulated biological pathways. *Transl. Psychiatry* **4,** e433 (2014).

32. James, S. J., Shpyleva, S., Melnyk, S., Pavliv, O. & Pogribny, I. P. Elevated 5-hydroxymethylcytosine in the Engrailed-2 (EN-2) promoter is associated with increased gene expression and decreased MeCP2 binding in autism cerebellum. *Transl. Psychiatry* **4,** e460 (2014).

33. Ladd-Acosta, C. *et al.* Common DNA methylation alterations in multiple brain regions in autism. *Mol. Psychiatry* **19,** 862–871 (2014).

34. Feinberg, J. I. *et al.* Paternal sperm DNA methylation associated with early signs of autism risk in an autism-enriched cohort. *Int. J. Epidemiol.* **44,** 1199–1210 (2015).

35. Smith, A. K. *et al.* Methylation quantitative trait loci (meQTLs) are consistently detected across ancestry, developmental stage, and tissue type. *BMC Genomics* **15,** 145 (2014).

36. Estes, M. L. & McAllister, A. K. Immune mediators in the brain and peripheral tissues in autism spectrum disorder. *Nat. Rev. Neurosci.* **16,** 469–486 (2015).

37. Voineagu, I. *et al.* Transcriptomic analysis of autistic brain reveals convergent molecular pathology. *Nature* **474,** 380–384 (2011).

bioRxiv preprint doi: https://doi.org/10.1101/091330; this version posted December 5, 2016. The copyright holder for this preprint (which was not certified by peer review) is the author/funder, who has granted bioRxiv a license to display the preprint in perpetuity. It is made available under aCC-BY 4.0 International license.

38. Gupta, S. *et al.* Transcriptome analysis reveals dysregulation of innate immune response genes and neuronal activity-dependent genes in autism. *Nat. Commun.* **5,** 5748 (2014).

39. Ander, B. P., Barger, N., Stamova, B., Sharp, F. R. & Schumann, C. M. Atypical miRNA expression in temporal cortex associated with dysregulation of immune, cell cycle, and other pathways in autism spectrum disorders. *Mol. Autism* **6,** 37 (2015).

40. Kong, S. W. *et al.* Peripheral blood gene expression signature differentiates children with autism from unaffected siblings. *Neurogenetics* **14,** 143–152 (2013).

41. Jalbrzikowski, M. *et al.* Transcriptome Profiling of Peripheral Blood in 22q11.2 Deletion Syndrome Reveals Functional Pathways Related to Psychosis and Autism Spectrum Disorder. *PloS One* **10,** e0132542 (2015).

42. O'Rawe, J. A. *et al.* TAF1 Variants Are Associated with Dysmorphic Features, Intellectual Disability, and Neurological Manifestations. *Am. J. Hum. Genet.* **97,** 922–932 (2015).

43. Baris, S. *et al.* Severe Early-Onset Combined Immunodeficiency due to Heterozygous Gain-of-Function Mutations in STAT1. *J. Clin. Immunol.* (2016). doi:10.1007/s10875-016-0312-3

44. Newschaffer, C. J. *et al.* Infant siblings and the investigation of autism risk factors. *J. Neurodev. Disord.* **4,** 7 (2012).

45. Aryee, M. J. *et al.* Minfi: a flexible and comprehensive Bioconductor package for the analysis of Infinium DNA methylation microarrays. *Bioinforma. Oxf. Engl.* **30,** 1363–1369 (2014).

46. Fortin, J.-P. *et al.* Functional normalization of 450k methylation array data improves replication in large cancer studies. *Genome Biol.* **15,** 503 (2014).

bioRxiv preprint doi: https://doi.org/10.1101/091330; this version posted December 5, 2016. The copyright holder for this preprint (which was not certified by peer review) is the author/funder, who has granted bioRxiv a license to display the preprint in perpetuity. It is made available under aCC-BY 4.0 International license.

47. Triche, T. J., Weisenberger, D. J., Van Den Berg, D., Laird, P. W. & Siegmund, K. D. Low-level processing of Illumina Infinium DNA Methylation BeadArrays. *Nucleic Acids Res.* **41,** e90 (2013).

48. Chen, Y. *et al.* Discovery of cross-reactive probes and polymorphic CpGs in the Illumina Infinium HumanMethylation450 microarray. *Epigenetics* **8,** 203–209 (2013).

49. Johnson, W. E., Li, C. & Rabinovic, A. Adjusting batch effects in microarray expression data using empirical Bayes methods. *Biostat. Oxf. Engl.* **8,** 118–127 (2007).

50. sva. *Bioconductor* Available at: http://bioconductor.org/packages/sva/. (Accessed: 5th August 2016)

51. 1000 Genomes Project Consortium *et al.* An integrated map of genetic variation from 1,092 human genomes. *Nature* **491,** 56–65 (2012).

52. Delaneau, O., Zagury, J.-F. & Marchini, J. Improved whole-chromosome phasing for disease and population genetic studies. *Nat. Methods* **10,** 5–6 (2013).

53. Howie, B., Fuchsberger, C., Stephens, M., Marchini, J. & Abecasis, G. R. Fast and accurate genotype imputation in genome-wide association studies through pre-phasing. *Nat. Genet.* **44,** 955–959 (2012).

54. Schendel, D. E. *et al.* The Study to Explore Early Development (SEED): a multisite epidemiologic study of autism by the Centers for Autism and Developmental Disabilities Research and Epidemiology (CADDRE) network. *J. Autism Dev. Disord.* **42,** 2121–2140 (2012).

bioRxiv preprint doi: https://doi.org/10.1101/091330; this version posted December 5, 2016. The copyright holder for this preprint (which was not certified by peer review) is the author/funder, who has granted bioRxiv a license to display the preprint in perpetuity. It is made available under aCC-BY 4.0 International license.

55. Touleimat, N. & Tost, J. Complete pipeline for Infinium(®) Human Methylation 450K BeadChip data processing using subset quantile normalization for accurate DNA methylation estimation. *Epigenomics* **4,** 325–341 (2012).

56. Price, A. L. *et al.* Principal components analysis corrects for stratification in genome-wide association studies. *Nat. Genet.* **38,** 904–909 (2006).

57. Gauderman, W. J. Sample Size Requirements for Association Studies of Gene-Gene Interaction. *Am. J. Epidemiol.* **155,** 478–484 (2002).

58. Shabalin, A. A. Matrix eQTL: ultra fast eQTL analysis via large matrix operations. *Bioinforma. Oxf. Engl.* **28,** 1353–1358 (2012).

59. Robinson, E. B. *et al.* Genetic risk for autism spectrum disorders and neuropsychiatric variation in the general population. *Nat. Genet.* **48,** 552–555 (2016).

60. Johnson, A. D. *et al.* SNAP: a web-based tool for identification and annotation of proxy SNPs using HapMap. *Bioinforma. Oxf. Engl.* **24,** 2938–2939 (2008).

61. PriorityPruner. Available at: http://prioritypruner.sourceforge.net/. (Accessed: 5th August 2016)

62. Bibikova, M. *et al.* High density DNA methylation array with single CpG site resolution. *Genomics* **98,** 288–295 (2011).

63. McClay, J. L. *et al.* High density methylation QTL analysis in human blood via next-generation sequencing of the methylated genomic DNA fraction. *Genome Biol.* **16,** 291 (2015).

64. missMethyl. *Bioconductor* Available at: http://bioconductor.org/packages/missMethyl/. (Accessed: 5th August 2016)

bioRxiv preprint doi: https://doi.org/10.1101/091330; this version posted December 5, 2016. The copyright holder for this preprint (which was not certified by peer review) is the author/funder, who has granted bioRxiv a license to display the preprint in perpetuity. It is made available under aCC-BY 4.0 International license.

65. Supek, F., Bošnjak, M., Škunca, N. & Šmuc, T. REVIGO summarizes and visualizes long lists of gene ontology terms. *PloS One* **6,** e21800 (2011).

66. Karolchik, D. *et al.* The UCSC Table Browser data retrieval tool. *Nucleic Acids Res.* **32,** D493-496 (2004).

67. IlluminaHumanMethylation450kmanifest. *Bioconductor* Available at: http://bioconductor.org/packages/IlluminaHumanMethylation450kmanifest/. (Accessed: 5th August 2016)

68. Edgar, R., Domrachev, M. & Lash, A. E. Gene Expression Omnibus: NCBI gene expression and hybridization array data repository. *Nucleic Acids Res.* **30,** 207–210 (2002).

69. Roadmap Epigenomics Consortium *et al.* Integrative analysis of 111 reference human epigenomes. *Nature* **518,** 317–330 (2015).

70. ENCODE Project Consortium. An integrated encyclopedia of DNA elements in the human genome. *Nature* **489,** 57–74 (2012).

ACKNOWLEDGEMENTS

We thank Eilis Hannon and Jonathan Mill for sharing the complete list of SNPs and 450k probes tested in their fetal brain meQTL analysis. We thank Jianxin Shi for sharing the same list from his lung meQTL study. S. Andrews was supported by the Burroughs-Wellcome Trust training grant: Maryland, Genetics, Epidemiology and Medicine (MD-GEM). The EARLI study was supported by NIEHS R01ES016443 and Autism Speaks grant #260377. The SEED study was supported in part by Autism Speaks #7659, NIEHS (R01ES01901; R01ES017646), and the

bioRxiv preprint doi: https://doi.org/10.1101/091330; this version posted December 5, 2016. The copyright holder for this preprint (which was not certified by peer review) is the author/funder, who has granted bioRxiv a license to display the preprint in perpetuity. It is made available under aCC-BY 4.0 International license.

Centers for Disease Control and Prevention (U10DD000180, U10DD000181, U10DD000182, U10DD000183, U10DD000184, U10DD000498).

AUTHOR CONTRIBUTIONS

C.L.A. and M.D.F. conceived the study. M.D.F., C.J.N., L.I.C., and I.H.P. led participation recruitment and sample selection for the EARLI study. S.V.A. performed quality control and processing for peripheral blood methylation data. B.S. and C.L.A. performed quality control for peripheral blood genotype data. K.M.B. performed quality control and processing for cord blood methylation and cord blood genotype data. S.V.A. designed meQTL parameter selection process, performed the meQTL queries, and implemented the FDR estimation. S.V.A. and S.E.E. designed and conducted all SNP and CpG-based enrichment analyses. S.V.A. designed and conducted GWAS loci expansion analysis. D.E.A, C.L.A, and M.D.F. supervised all analyses. S.V.A, S.E.E., K.M.B., C.L.A, and M.D.F. contributed to writing the manuscript. All authors contributed to interpretation of results and edited and reviewed the manuscript.

COMPETING FINANCIAL INTERESTS

The authors declare no competing financial interests.

Correspondence to: **Christine Ladd-Acosta, PhD,** Wendy Klag Center for Autism and Developmental Disabilities, Johns Hopkins Bloomberg School of Public Health, 615 N. Wolfe St, E6518, Baltimore, MD 21205, Email: claddac1@jhu.edu

bioRxiv preprint doi: https://doi.org/10.1101/091330; this version posted December 5, 2016. The copyright holder for this preprint (which was not certified by peer review) is the author/funder, who has granted bioRxiv a license to display the preprint in perpetuity. It is made available under aCC-BY 4.0 International license.

or **M. Daniele Fallin, PhD**, Wendy Klag Center for Autism and Developmental Disabilities, Johns Hopkins Bloomberg School of Public Health, 624 N. Broadway, HH850, Baltimore, MD, 21205, USA, Email: dfallin@jhu.edu

FIGURES

Figure 1: Specific interrogation of ASD-related PGC loci with evidence for meQTLs in peripheral blood, cord blood, and fetal brain. These plots allow for a visual evaluation of the nature of SNP and CpG correlation structure together with meQTL relationships and the additional genes they implicate, in multiple tissues simultaneously. Locus coordinates differ from those in **Supplementary Data 6** because in this context they encompass the locations of CpG sites implicated via meQTL associations. From bottom panel to top: linkage disequilibrium (LD) plot of SNPs in specified locus region and genes mapping to the region via the UCSC genome browser. Then for each tissue: meQTL association lines connecting SNP (bottom of line) to CpG site with which it is associated (top of line), at FDR 5% in peripheral blood and cord blood and past 1e-08 p-value threshold in fetal brain results; lines mapping CpG sites to where they are located in the region (bottom of line) to where they are positioned in the CpG-CpG correlation plot. Red meQTL association lines denote SNP-CpG associations where the SNP is ASD-associated in PGC (p-value <= 1e-04); gray meQTL association lines denote all other SNP to CpG associations reported in that tissue/dataset. **Panel A**) Locus chr8:10789493-10789493 (row 1) from Table 3. **Panel B**) Locus chr19:49646006-49647618 (row 2) from Table 3.

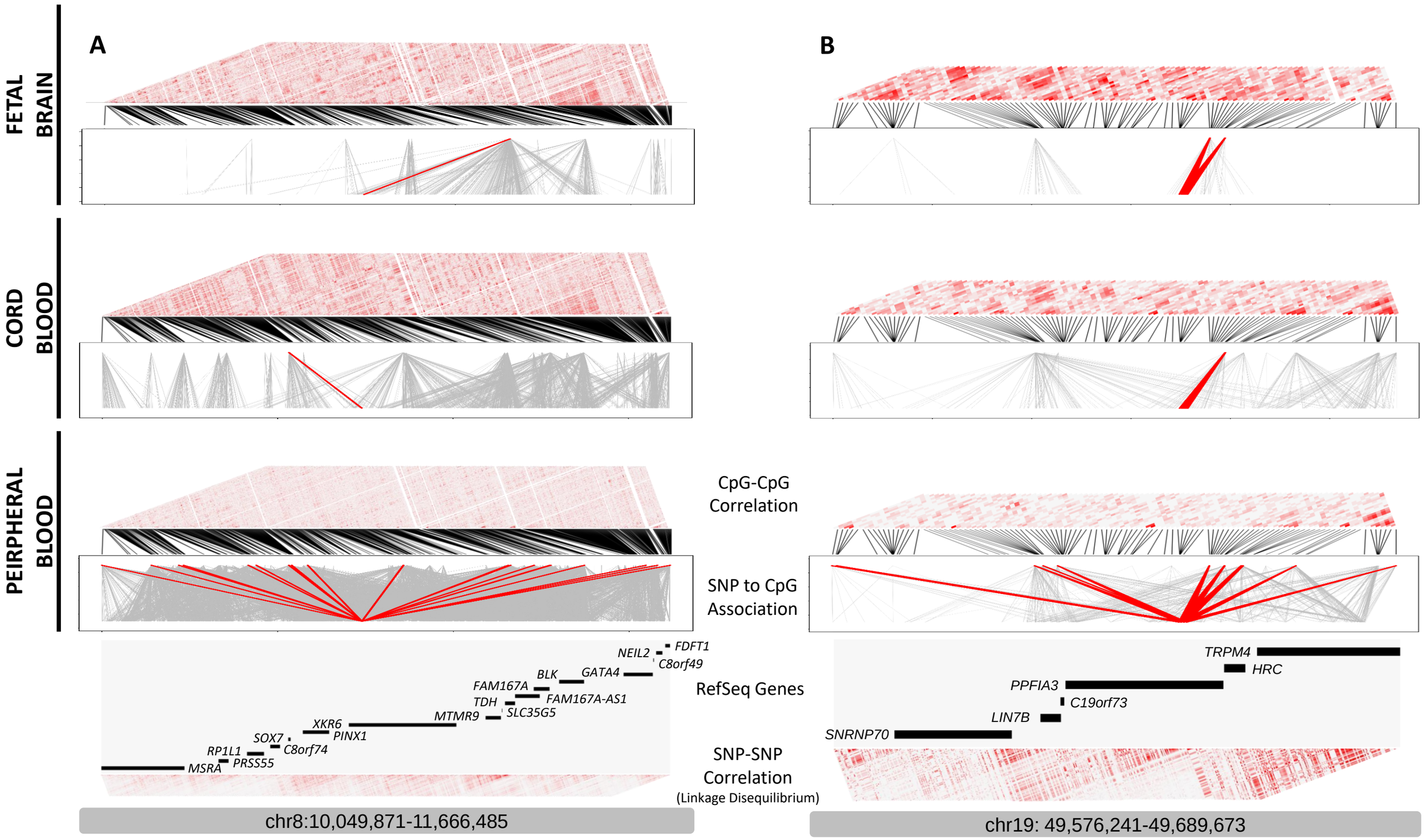

r^2/Correlation

0 0.2 0.4 0.6 0.8 1

Value

Non-ASD SNP to CpG association
PB p-value <= 1.1E-5 = FDR 5%
CB p-value <= 2.7E-6 = FDR 5%
FB p-value < 1E-8

ASD SNP to CpG association
PB p-value <= 1.1E-5 = FDR 5%
CB p-value <= 2.7E-6 = FDR 5%
FB p-value < 1E-8

bioRxiv preprint doi: https://doi.org/10.1101/091330; this version posted December 5, 2016. The copyright holder for this preprint (which was not certified by peer review) is the author/funder, who has granted bioRxiv a license to display the preprint in perpetuity. It is made available under aCC-BY 4.0 International license.

Figure 2: Enrichment of meQTL target CpG sites in DNaseI hypersensitive sites. We identified the meQTL targets (at FDR 5% in peripheral blood, cord blood, and lung and past 1e-08 p-value threshold in fetal brain results) in peripheral blood, cord blood, fetal brain and lung as well those meQTL targets that were present in the overlap of peripheral blood with the other three tissues. Odds ratio and p-value in gray text represent enrichment fold statistic and p-value from Fisher's exact tests examining the tendency of meQTL targets to overlap with DHS sites compared to CpG sites that were not meQTL targets. Odds ratio and p-value in black text represent enrichment fold statistic and p-value from Fisher's exact tests examining the tendency of meQTL targets of significant (p-value <= 1e-04) SNPs from the PGC cross-disorder results or their proxies (r^2 >= 0.8) to overlap with DHS sites compared to CpG sites that were not meQTL targets of the same SNPs. A full list of enrichment statistics and p-value for both tests against a total of 181 cell-type specific DHS sites, cell-type specific chromatin marks, and transcription factor binding sites is available in **Supplementary Data 7 and 8**.

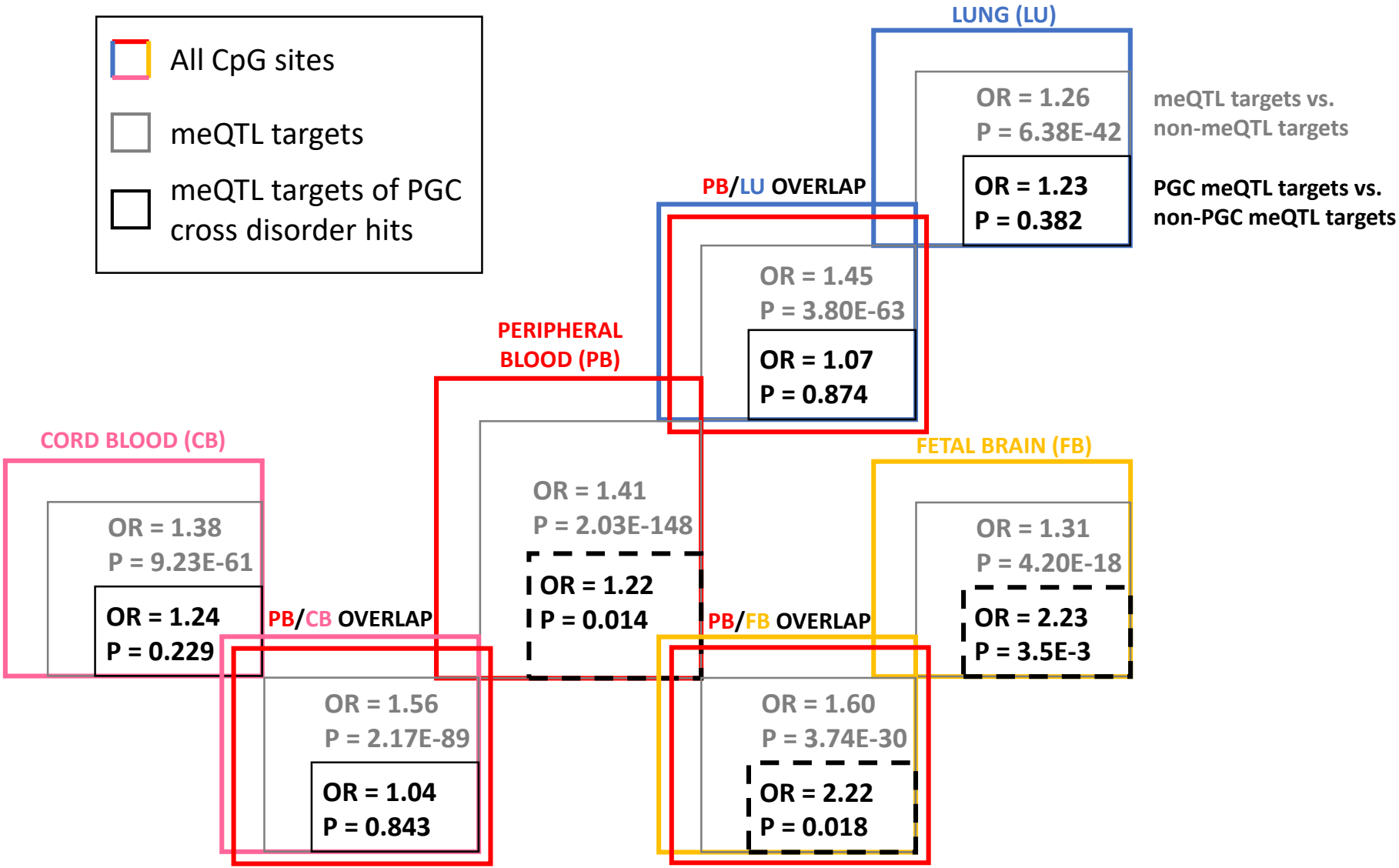
All CpG sites
meQTL targets
meQTL targets of PGC cross disorder hits
LUNG (LU)
OR = 1.26
P = 6.38E-42
OR = 1.23
P = 0.382
meQTL targets vs. non-meQTL targets
PGC meQTL targets vs. non-PGC meQTL targets
PB/LU OVERLAP
OR = 1.45
P = 3.80E-63
OR = 1.07
P = 0.874
PERIPHERAL BLOOD (PB)
CORD BLOOD (CB)
OR = 1.38
P = 9.23E-61
OR = 1.24
P = 0.229
OR = 1.41
P = 2.03E-148
OR = 1.22
P = 0.014
FETAL BRAIN (FB)
OR = 1.31
P = 4.20E-18
OR = 2.23
P = 3.5E-3
PB/CB OVERLAP
PB/FB OVERLAP
OR = 1.56
P = 2.17E-89
OR = 1.04
P = 0.843
OR = 1.60
P = 3.74E-30
OR = 2.22
P = 0.018

TABLES

Table 1: Descriptive characteristics, meQTL query parameters, and meQTL summary results for 4 tissues examined.

	Sample Size	*Meth SD Cutoff* [b]	*SNP MAF Threshold* [c]	*Max SNP to CpG Distance*[d]	*meQTL p-value thresholds* [e]	*# of meQTLs identified*	*# of meQTL targets identified*
Fetal Brain[a]	166	NA	5%	1 Mb	1.0e-08[f]	299 992[f]	7 863[f]
Peripheral Blood	339	0.15	2.75%	1 Mb	3.1e-05[g] 1.0e-05[h] 3.0e-07[i]	2 003 443[g] 1 878 577[h] 1 598 033[i]	95 195[g] 85 250[h] 68 860[i]
Cord Blood	121	0.15	7%	500 Kb	8.5e-06[g] 2.7e-06[h] 2.0e-07[i]	1 374 554[g] 1 252 498[h] 1 032 370[i]	41 681[g] 35 905[h] 28 423[i]
Lung[a]	210	NA	3%	500 Kb	4.0e-05[h]	22 866[h]	34 304[h]

[a]Publicly available data. [b]The probe standard deviation across samples that was used as an inclusion criterion for probes in the meQTL query (blood datasets only). [c]The MAF cutoff used as inclusion criterion for SNPs in the meQTL query. [d]The maximum distance between the SNP and CpG site used in the meQTL query for the peripheral blood, cord blood, and lung datasets, and the value at which results for filtered in the fetal brain results. [e]The peripheral blood, cord blood, and lung datasets the p-values calculated to control the FDR at various rates (see Materials and Methods). [f]FDR not specified. [g]FDR = 10% [h]FDR = 5% [i]FDR = 1%

Table 2: Enrichment statistics for meQTLs derived from 4 tissue types in ASD GWAS SNPs.

	ASD p-value = 1e-03			**ASD p-value = 1e-04**		
	meQTL p-value = 1e-08			***meQTL p-value = 1e-08***		
Fetal Brain[1]	1.70 (<0.001)			3.55 (<0.001)		
	meQTL FDR = 10%	***meQTL FDR = 5%***	***meQTL FDR = 1%***	***meQTL FDR = 10%***	***meQTL FDR = 5%***	***meQTL FDR = 1%***
Peripheral Blood[2]	1.22 (< 0.001)	1.20 (< 0.001)	1.23 (< 0.001)	1.31 (0.001)	1.40 (< 0.001)	1.58 (< 0.001)
Cord Blood[2]	1.14 (0.032)	1.21 (0.011)	1.20 (0.023)	1.13 (0.299)	1.10 (0.392)	1.10 (0.406)
Lung[1]	-	1.09 (0.343)	-	-	0.80 (0.301)	-

Enrichment fold statistics and p-values based 1,000 permutations are reported. [1]LD pruning performed with 1000 Genomes CEU samples. [2]LD pruning performed with study-specific genotype data.

bioRxiv preprint doi: https://doi.org/10.1101/091330; this version posted December 5, 2016. The copyright holder for this preprint (which was not certified by peer review) is the author/funder, who has granted bioRxiv a license to display the preprint in perpetuity. It is made available under aCC-BY 4.0 International license.

Table 3: Gene Ontology terms significantly enriched in multiple tissue types in comparison of ASD-related meQTL targets to meQTL targets generally.

Term	Peripheral Blood Scaled Rank[1]	Cord Blood Scaled Rank[1]	Fetal Brain Scaled Rank[1]
response to interferon-gamma	0.14	0.11	0.11
positive regulation of relaxation of cardiac muscle	0.20	0.46	0.30
production of molecular mediator of immune response	0.65	0.22	0.28
cellular response to interferon-gamma	NA	0.07	0.09
detection of bacterium	NA	0.18	0.06
detection of biotic stimulus	NA	0.26	0.04
T-helper 1 type immune response	NA	0.08	0.34
regulation of interleukin-10 secretion	NA	0.09	0.43
interferon-gamma production	NA	0.57	0.19
regulation of interleukin-4 production	NA	0.24	0.62
interleukin-4 production	NA	0.29	0.60
interleukin-10 production	NA	0.25	0.74
tongue development	NA	0.68	0.32
inflammatory response to antigenic stimulus	NA	0.32	0.81
endochondral bone growth	NA	0.71	0.53
antigen processing and presentation of peptide or polysaccharide antigen via MHC class II	0.01	0.05	NA
T cell costimulation	0.05	0.01	NA
positive regulation of hormone secretion	0.09	0.04	NA
antigen receptor-mediated signaling pathway	0.08	0.13	NA
immunoglobulin production involved in immunoglobulin mediated immune response	0.24	0.03	NA
single organismal cell-cell adhesion	0.23	0.12	NA
single organism cell adhesion	0.34	0.16	NA
negative regulation of nonmotile primary cilium assembly	0.16	0.39	NA
antigen processing and presentation of polysaccharide antigen via MHC class II	0.02	0.58	NA
polysaccharide assembly with MHC class II protein complex	0.03	0.59	NA
protein-carbohydrate complex subunit organization	0.04	0.61	NA
microtubule sliding	0.29	0.38	NA
MHC protein complex assembly	0.06	0.75	NA
negative regulation of serine-type peptidase activity	0.41	0.41	NA
regulation of satellite cell activation involved in skeletal muscle regeneration	0.39	0.45	NA
protein repair	0.43	0.43	NA
regulation of serine-type peptidase activity	0.48	0.47	NA
protein localization to basolateral plasma membrane	0.46	0.55	NA

1

bioRxiv preprint doi: https://doi.org/10.1101/091330; this version posted December 5, 2016. The copyright holder for this preprint (which was not certified by peer review) is the author/funder, who has granted bioRxiv a license to display the preprint in perpetuity. It is made available under aCC-BY 4.0 International license.

lymphocyte migration into lymphoid organs	0.47	0.62	NA
Peyer's patch morphogenesis	0.60	0.70	NA
regulation of homeostatic process	0.45	0.92	NA
skeletal muscle satellite cell activation	0.88	0.63	NA

[1]: Scaled rank refers to enrichment p-value based rank divided by the number of marginally significant terms post REVIGO filtering for that tissue (peripheral blood: 95, cord blood: 76, fetal brain: 47). 'NA' shown for terms that did appear in these lists for that tissue. Terms are lumped into groups based on cross-tissue overlap: all three tissues, cord blood and fetal brain, peripheral blood and cord blood. Within each of these groups terms are arranged according to the sum of the scaled ranks. See methods for more details.

SUPPLEMENTARY FILES

Supplementary Information: Supplementary Figures 1-4 and Supplementary Tables 1-2.

Supplementary Data 1: Peripheral blood meQTLs identified at FDR = 5%. Available at http://www.arkinglab.org/resources/

Supplementary Data 2: Cord blood meQTLs identified at FDR = 5%. Available at http://www.arkinglab.org/resources/

Supplementary Data 3: Marginally significant Gene Ontology Terms post REVIGO comparing ASD-related meQTL targets to meQTL targets generally in peripheral blood.

Supplementary Data 4: Marginally significant Gene Ontology Terms post REVIGO comparing ASD-related meQTL targets to meQTL targets generally in cord blood.

Supplementary Data 5: Marginally significant Gene Ontology Terms post REVIGO comparing ASD-related meQTL targets to meQTL targets generally in fetal brain.

Supplementary Data 6: meQTL evidence for every ASD-associated (PGC p-value < 1E-4) locus.

Supplementary Data 7: Enrichment Statistics comparing meQTL targets of cross-disorder PGC SNPs to meQTL targets of non cross disorder PGC associated SNPs with respect to regulatory feature overlap.

Supplementary Data 8: Enrichment Statistics comparing meQTL targets to non-meQTL targets with respect to regulatory feature overlap.

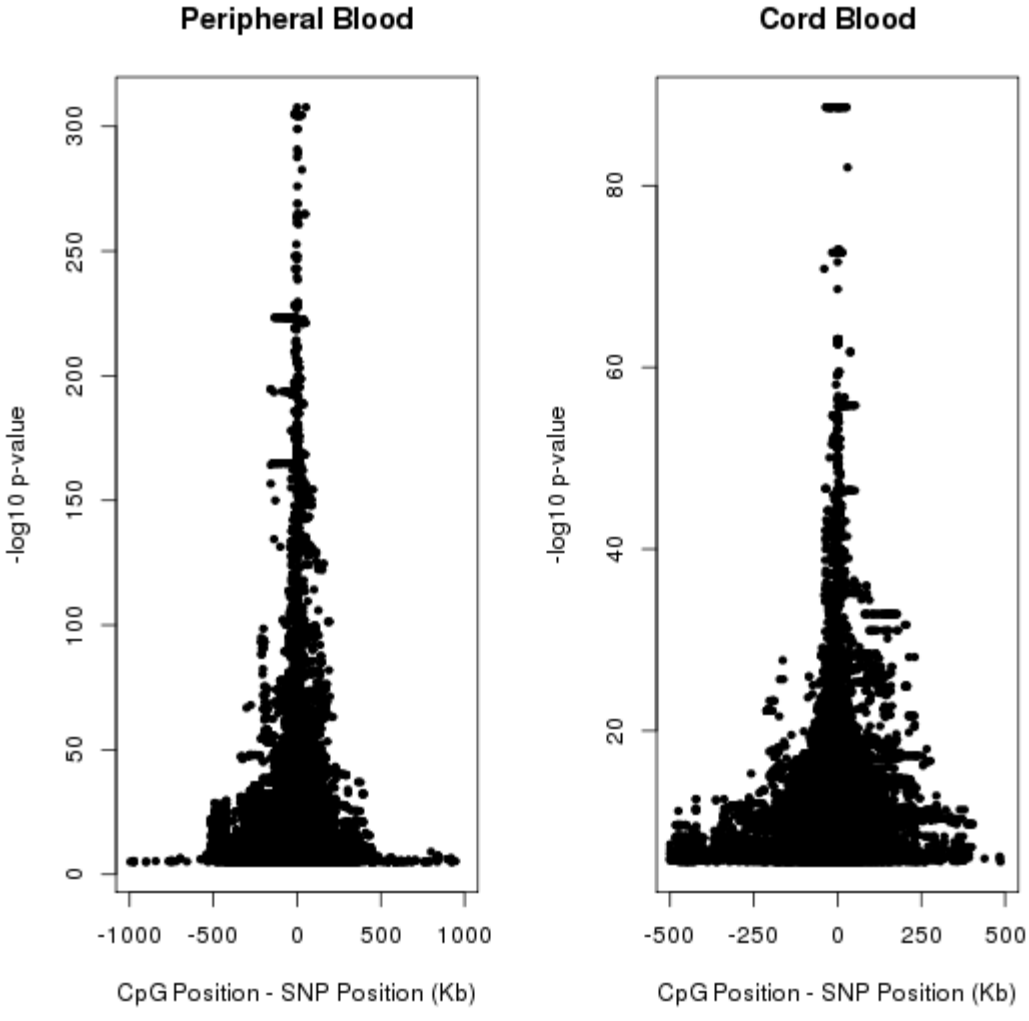

Supplementary Figure 1: **The relationship between degree of significance and distance between SNP and CpG site on chromosome 21.** Degree of significance (y-axis) defined by -log10 p-value. Only meQTLs present at FDR = 5% are shown. The degree of significance decays with increasing distance. Left panel shows relationship for SEED peripheral blood data and right panel shows relationship for EARLI cord blood data.

bioRxiv preprint doi: https://doi.org/10.1101/091330; this version posted December 5, 2016. The copyright holder for this preprint (which was not certified by peer review) is the author/funder, who has granted bioRxiv a license to display the preprint in perpetuity. It is made available under aCC-BY 4.0 International license.

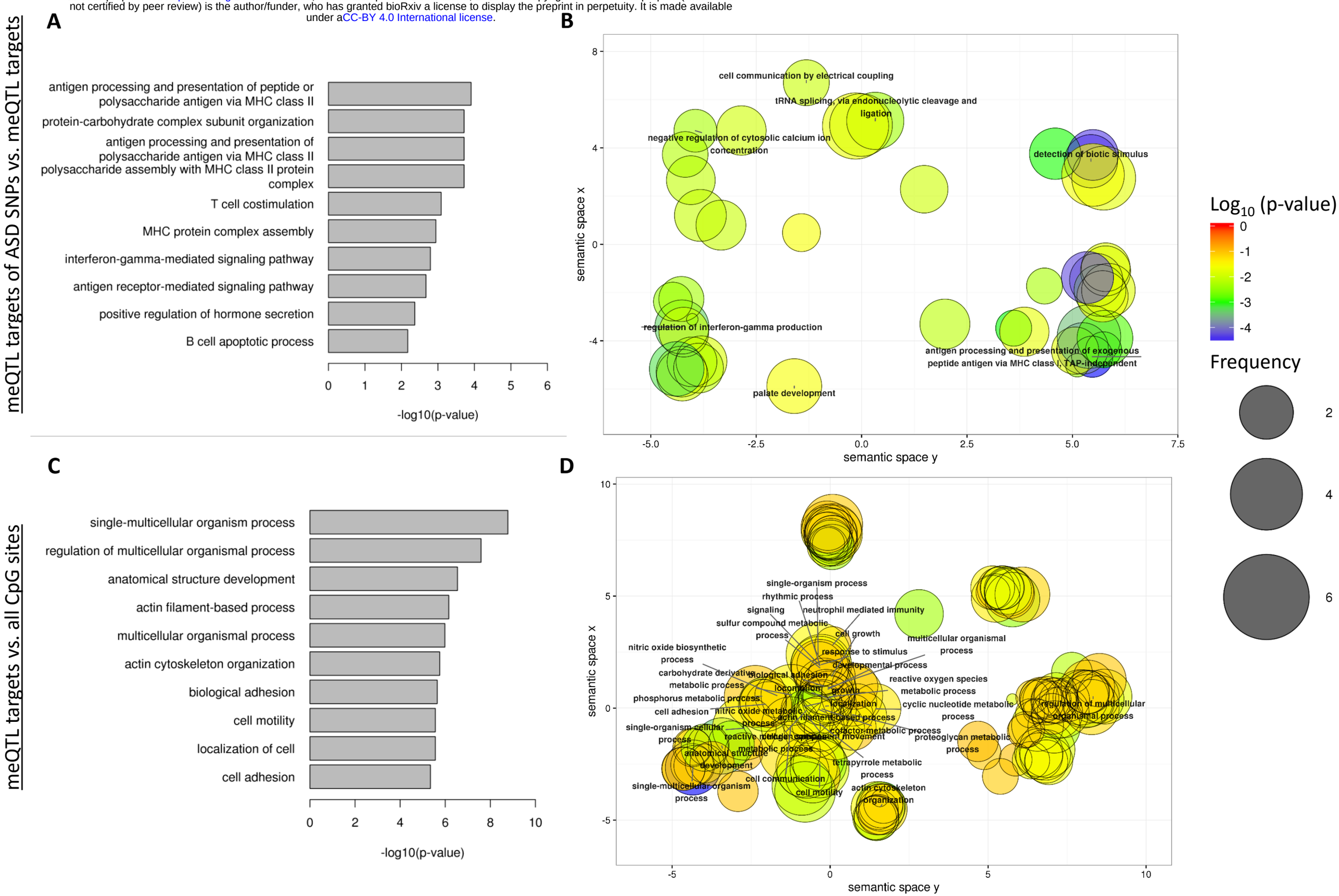

Supplementary Figure 2: **Gene Ontology enrichment analysis for meQTL targets in peripheral blood.** Gene Ontology (GO) enrichment analysis via the 'gometh' function in the *MissMethyl* R package. The results for the "biological processes" group were pruned to remove overlapping terms using the REVIGO software. Results shown for meQTL targets of ASD-related (PGC p-value < 1E-4) SNPs and their proxies (r^2) against a background of all meQTL targets (n = 201 vs n = 59,308; **Panels A+B**) and for meQTL targets against a background of all CpG sties tested (n = 59,308 vs n = 290,066; **Panels C+D**). meQTL targets all defined via meQTL p-value threshold = FDR 5%. **Panels A+C**) The top 10 biological process by GO enrichment p-value after REVIGO pruning. **Panel B+D**) A multi-dimensional scaling projection of the semantic similarity in nominally significant (enrichment p-value < 0.05) GO terms produced by REVIGO. Clusters are identified via labeling of the terms with both the least redundancy and highest degree of enrichment ('dispensability' value < 0.15). Color reflect degree of significance and increasing size reflects greater frequency of term in GO database.

bioRxiv preprint doi: https://doi.org/10.1101/091330; this version posted December 5, 2016. The copyright holder for this preprint (which was not certified by peer review) is the author/funder, who has granted bioRxiv a license to display the preprint in perpetuity. It is made available under aCC-BY 4.0 International license.

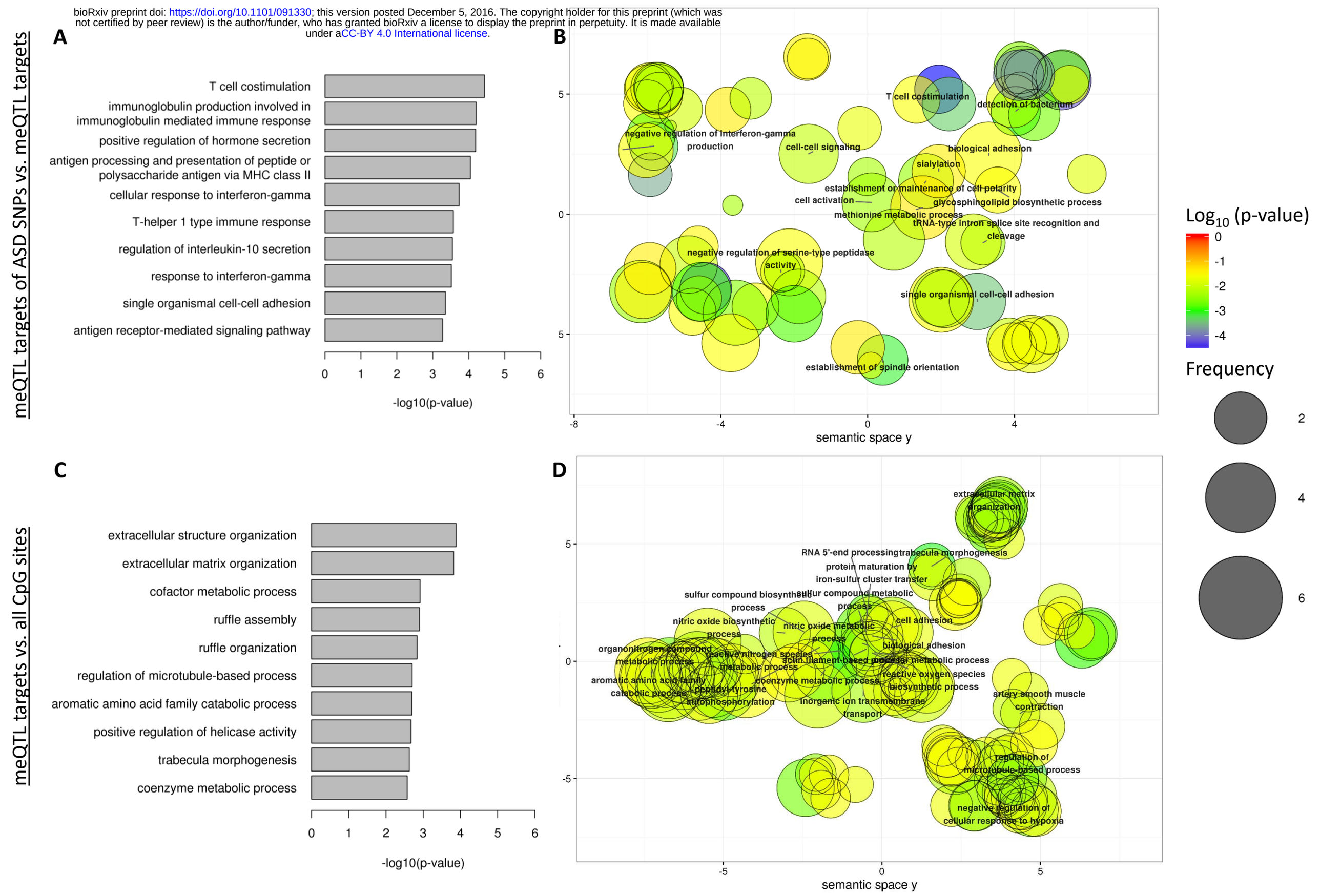

Supplementary Figure 3: **Gene Ontology enrichment analysis for meQTL targets in cord blood.** Gene Ontology (GO) enrichment analysis via the 'gometh' function in the *MissMethyl* R package. The results for the "biological processes" group were pruned to remove overlapping terms using the REVIGO software. Results shown for meQTL targets of ASD-related (PGC p-value < 1E-4) SNPs and their proxies (r^2) against a background of all meQTL targets (n = 66 vs n = 22,803; **Panels A+B**) and for meQTL targets against a background of all CpG sties tested (n = 22,803 vs n = 289,645; **Panels C+D**). meQTL targets all defined via meQTL p-value threshold = FDR 5%. **Panels A+C**) The top 10 biological process by GO enrichment p-value after REVIGO pruning. **Panel B+D**) A multi-dimensional scaling projection of the semantic similarity in nominally significant (enrichment p-value < 0.05) GO terms produced by REVIGO. Clusters are identified via labeling of the terms with both the least redundancy and highest degree of enrichment ('dispensability' value < 0.15). Color reflect degree of significance and increasing size reflects greater frequency of term in GO database.

bioRxiv preprint doi: https://doi.org/10.1101/091330; this version posted December 5, 2016. The copyright holder for this preprint (which was not certified by peer review) is the author/funder, who has granted bioRxiv a license to display the preprint in perpetuity. It is made available under aCC-BY 4.0 International license.

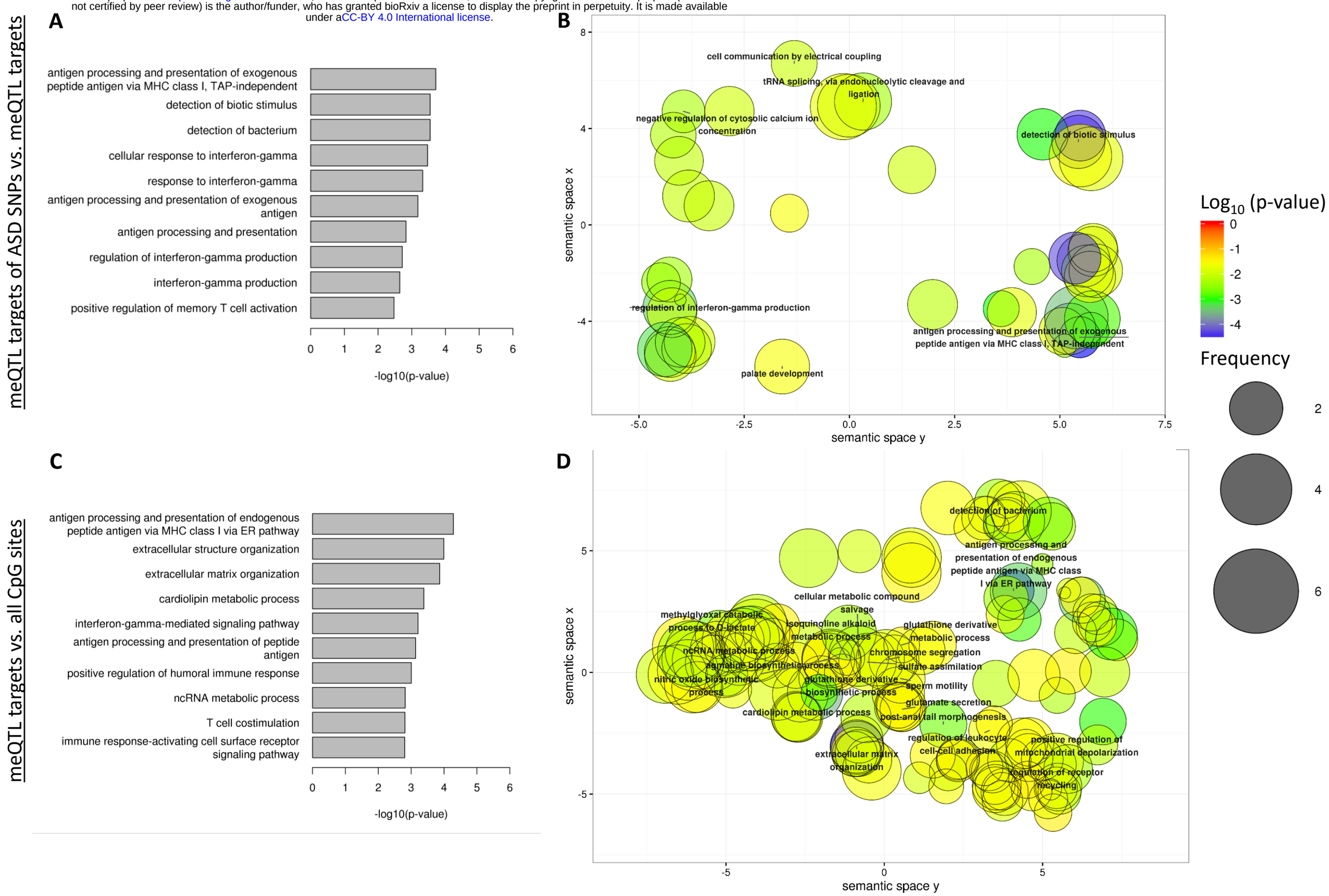

Supplementary Figure 4: **Gene Ontology enrichment analysis for meQTL targets in fetal brain.** Gene Ontology (GO) enrichment analysis via the 'gometh' function in the *MissMethyl* R package. The results for the "biological processes" group were pruned to remove overlapping terms using the REVIGO software. Results shown for meQTL targets of ASD-related (PGC p-value < 1E-4) SNPs and their proxies (r^2) against a background of all meQTL targets (n = 53 vs n = 7,863; **Panels A+B**) and for meQTL targets against a background of all CpG sties tested (n = 7,863 vs n = 314,554; **Panels C+D**). meQTL targets all defined via meQTL p-value threshold = FDR 5%. **Panels A+C**) The top 10 biological process by GO enrichment p-value after REVIGO pruning. **Panel B+D**) A multi-dimensional scaling projection of the semantic similarity in nominally significant (enrichment p-value < 0.05) GO terms produced by REVIGO. Clusters are identified via labeling of the terms with both the least redundancy and highest degree of enrichment ('dispensability' value < 0.15). Color reflect degree of significance and increasing size reflects greater frequency of term in GO database.

Supplementary Table 1: Summary of meQTL evidence across tissue type.

Scenario	Blood	Cord Blood	Fetal Brain	SNPs	% of Total SNPs	Independent Sites	% of Total Independent Sites
1	✓	✓	✓	125,869	4.65%	6,640	4.15%
2	✓	✓	×	407,722	15.08%	22,135	13.83%
3	✓	×	✓	30,691	1.14%	1,354	0.85%
4	✓	×	×	722,703	26.73%	42,561	26.58%
5	×	✓	✓	528	0.02%	18	0.01%
6	×	✓	×	6,299	0.23%	333	0.21%
7	×	×	✓	4,940	0.18%	237	0.15%
8	×	×	×	1,405,261	51.97%	86,821	54.23%
			SUM	2,704,013		160,099	

Results are shown for meQTLs associated at FDR = 5% threshold in blood and cord blood datasets and threshold of 1E-8 in fetal brain.

Only SNPs that were included in all three tissues in their respective meQTL queries are included in this analyis (n = 2,704,013).

Independent sites were constructed by grouping SNPs into bins defined by recombination hot spot data from 1000 Genomes (see Methods).

For example, scenario 1 lists that there are a total of 125,869 SNPs that are meQTLs in blood, cord blood, and fetal brain, which fall into 6,640 loci.

Supplementary Table 2: Summary of meQTL evidence for PGC results.

Scenario	Blood	Cord Blood	Fetal Brain	SNPs	% of Total SNPs	Independent Sites	% of Total Independent Sites
1	✓	✓	✓	5	0.46%	2	0.80%
2	✓	✓	×	74	6.76%	18	7.23%
3	✓	×	✓	0	0.00%	0	0.00%
4	✓	×	×	195	17.82%	28	11.24%
5	×	✓	✓	19	1.74%	8	3.21%
6	×	✓	×	75	6.86%	13	5.22%
7	×	×	✓	0	0.00%	0	0.00%
8	×	×	×	726	66.36%	180	72.29%
			SUM	1094		249	

Results are shown for meQTLs associated at FDR = 5% threshold in blood and cord blood datasets and threshold of 1E-8 in fetal brain.
All SNPs in PGC, regardless of if they were tested in the respective meQTL studies, are included in this analysis.
Independent sites were constructed by grouping SNPs into bins defined by recombination hot spot data from 1000 Genomes (see Methods).
For example, scenario 1 lists that there are a total of 5 SNPs that are meQTLs in blood, cord blood, and fetal brain, which fall into 2 loci.